

# Supporting Material

## “Redox state of cytochromes in frozen yeast cells probed by resonance Raman spectroscopy”

Konstantin A. Okotrub and Nikolay V. Surovtsev\*

\*Corresponding author, email: [lab21@iae.nsk.su](mailto:lab21@iae.nsk.su)

Pr. Ak. Koptyuga 1, 630090, Novosibirsk, Russia

Tel. 7-383-3307978

### Raman lines assignment

In our Raman experiment the yeast cell suspension was placed between two silica glass plates or between a glass plate and a piece of mica (Materials and Methods of Article). Hence, Raman signal from the mica slice and/or the silica glass can contribute to the measured Raman spectra. To take into account these contributions the Raman scattering from the silica glass and the mica slice was studied. Raman spectra of the yeast cell in the sample installation, the silica glass and the mica slice measured at different temperatures are shown in Fig. S1. Figure S1 helps in the assignment of the experimental Raman lines. From Fig. S1 it is seen that the Raman spectra of the mica and silica weakly depend on temperature.

Raman spectrum of yeast cells averaged over the different scan during the measurements is shown in Fig. S1 at few representative temperatures. Temperature evolution of Raman spectrum relates to the change of the cytochrome contribution discussed in Article. Non-resonance Raman lines obey weak temperature dependences (Fig. S1). The assignment of Raman lines corresponding to the yeast cell is presented in Table S1.

Photoluminescence background in the measured spectra was corrected with a straight line. At room temperature the intensity of photoluminescence was

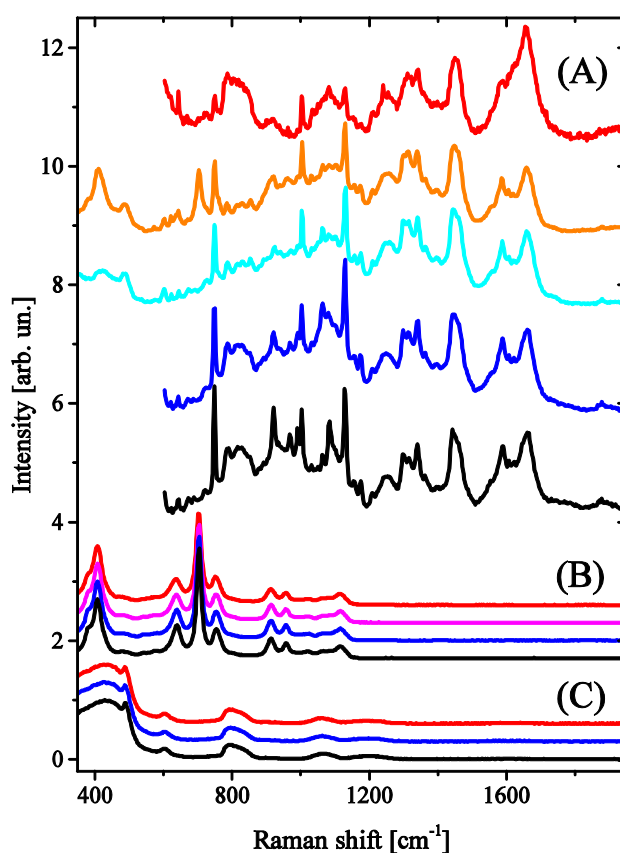


FIGURE S1. (A) Raman spectra of yeast cells in the sample installation of the Linkam cryostage at  $T = -30$  °C (the orange line) and in the sample installation of the vacuum cryostat at  $T = +25$  °C (the red line),  $-70$  °C (the cyan line),  $-100$  °C (the blue line),  $-173$  °C (the black line). (B) Raman spectra of a mica slice at  $T = +25, -30, -100, -180$  °C (from top to bottom). (C) Raman spectra of a silica glass at  $T = +25, -40, -170$  °C (from top to bottom). The spectra are vertically shifted for convenience.

somehow lower than the intensity of CH deformation mode. At -100 °C the photoluminescence was 50 times more intensive than at room temperature (for the first scan with 2 min exposition). However, the laser exposition leads to the photoluminescence background decrease. At -100 °C the photoluminescence decreases under irradiation by more than an order of magnitude.

TABLE S1. Raman lines assignment.

| Line position, $\text{cm}^{-1}$ | Assignment  |
|---------------------------------|---|
| 604                             | cytochrome <i>c</i> (1, 2)  |
| 622                             | phenylalanine (3)   |
| 645                             | tyrosine (3)  |
| 672                             | thymine (5)   |
| 688                             | cytochrome (2); guanine (5)   |
| 724                             | adenine (5)   |
| 749                             | cytochrome <i>c</i> and <i>b</i> (2)  |
| 786                             | cytosine, thymine (5)   |
| 814                             | RNA phosphate backbone (5,6)  |
| 830                             | phenylalanine (3)   |
| 852                             | tyrosine (3)  |
| 879                             | undetermined: possibly phosphate backbone (5)                                     |
| 892, 905                        | rocking $\text{CH}_2$ (3,4)   |
| 922, 970, 992                   | cytochrome <i>c</i> and <i>b</i> (2)  |
| 1004                            | phenylalanine (3,7)   |
| 1032                            | phenylalanine (3,7)   |
| 1050                            | C - O (4,5)   |
| 1064, 1081, 1102                | saturated compounds (C-C) (3)   |
| 1129, 1155, 1176                | cytochrome <i>c</i> and <i>b</i> (2)  |
| 1210                            | phenylalanine, tyrosine (7)   |
| 1250 (broad)                    | saccharides, aminoacides, nucleotides (3)   |
| 1300                            | twisting $\text{CH}_2$ (3); cytochrome <i>c</i> and <i>b</i> (2); amide III (4,7) |
| 1315, 1341                      | cytochrome <i>c</i> and <i>b</i> (2)  |
| 1392                            | deoxyribose phosphate backbone $\delta(\text{CH}_2)$ , guanine (3,5)              |
| 1450 (broad)                    | scissoring $\text{CH}_2$ , umbrella $\text{CH}_3$ modes (4)                       |
| 1552                            | amide II (4)  |
| 1587                            | cytochrome <i>c</i> and <i>b</i> (2); phenylalanine (3)                           |
| 1606, 1619                      | undetermined: C = C or aromatic $\text{C} \equiv \text{C}$ (4)                    |
| 1655 (multicomponent)           | amide I ( $1650 \text{ cm}^{-1}$ ) and other C = O, C = C (4)                     |
| 1734, 1877                      | C = O (4)   |

## Data processing

We followed the intensity ratio of  $749 \text{ cm}^{-1}$  and  $\delta\text{CH}$  Raman lines to estimate the reduced cytochrome amount in yeast cells. The way of the line intensities estimation is illustrated in Fig. S2. Intensity of the cytochrome peak at  $749 \text{ cm}^{-1}$  was quantified as a difference between the average of three pixels of maximal intensity and the baseline.

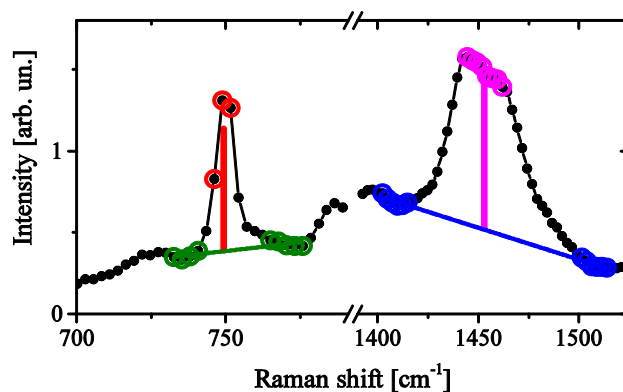


FIGURE S2. Quantification of the yeast Raman line intensities. The green and blue points denote the pixels used in the baseline interpolation, which are shown by the straight lines. The vertical lines demonstrate the intensity of the peaks quantified as described in the text.

The baseline was interpolated by a straight line between the pixels determining the peak background (Fig. S2). The similar calculations were used for the  $\delta\text{CH}$  mode (see Fig. S2), where the average of nine pixels of maximal intensity were used. This is equivalent to integration range of  $\sim 27 \text{ cm}^{-1}$ . The integration range minimizes the effect of temperature for the  $\delta\text{CH}$  mode (see Fig. 2 of Article). Where necessary the overlap of the cytochrome peak at  $749 \text{ cm}^{-1}$  with the mica spectrum was taken into account (the typical correction value was less than 10 % of the value of  $749 \text{ cm}^{-1}$  line at the beginning of the irradiation).

From 10 to 40 cells were studied at all considered experimental conditions depicted in Figs. 3 and 4 of Article. For every cell the experimental

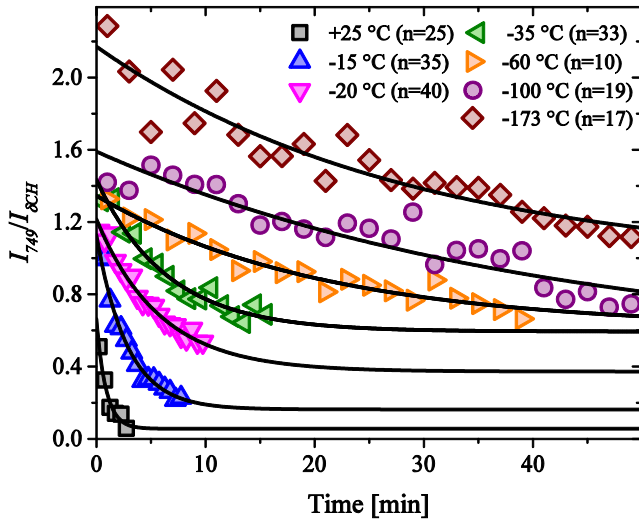


FIGURE S3. Time dependence of the  $I_{749}/I_{\delta CH}$  ratio at different temperatures ( $P = 2.4$  mW). Not all data are shown for the experiment at  $T = -100, -173$  °C; the total exposition time was 80 minutes in this case. The number of cells used in averaging is shown in brackets.

$I_{749}/I_{\delta CH}(t)$  ratio was fitted with decaying exponent (see Eq. 1). The average values of the parameters ( $\tau^{-1}$ ,  $y_0$ ,  $A$ ) discussed in Article were found from the arithmetical mean over the set of parameters of different cells. To verify the validity of the exponential decay fit the  $I_{749}/I_{\delta CH}(t)$  ratio with higher statistics was considered. In this case the  $I_{749}/I_{\delta CH}(t)$  ratio was found from averaging over Raman spectra of all cells studied. The time dependence of this ratio is shown in Fig. S3 at a few representative temperatures. It is seen that the exponential decay fit works well.

## Effect of ice formation

In one experiment the spontaneous ice formation occurred only after  $\sim 2$  hours of being at  $-20$  °C. Raman scattering measurement from single cells had been started before the ice formation and finished after that (Fig S4). The Raman measurement from the first 16 cells was done from the cells contained in supercooled solution. In this case the ratio  $I_{749}/I_{\delta CH}$  was about 0.1 for 4 minutes acquisition. After the ice formation the Raman measurements were performed from the cells trapped in the ice. The first one of them showed the  $I_{749}/I_{\delta CH}$  ratio similar to one measured before. Next measurements provided the average  $I_{749}/I_{\delta CH}=1.3$ . Fig. S4 demonstrates the effect of the spontaneous ice formation on the intensity of the cytochrome contribution. We estimated that the process of cytochrome reduction in cells had taken from 5 to 10 minutes.

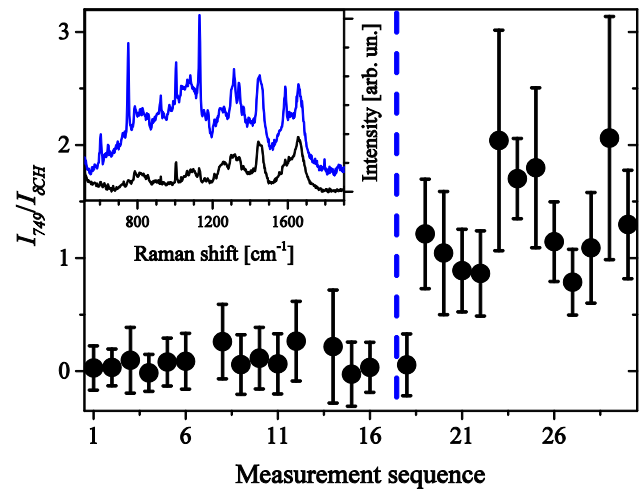


FIGURE S4. Effect of the ice formation on  $I_{749}/I_{\delta CH}$  ratio at  $T = -20$  °C. The black circles correspond to  $I_{749}/I_{\delta CH}$  ratio evaluated from the single cell measurements with 4 minutes exposition. The vertical line depicts the moment of ice formation in the experiment. The insert: the Raman spectra measured before and after ice formation.

## Arrhenius plot for $\alpha$ coefficient

Temperature dependence of the  $\alpha$  coefficient from Eq. (2) can be described by the sum of the thermal activation law and a constant, see Fig. 5.

$$\alpha(T) = \alpha_0 + q_0 e^{-U/RT} \quad (\text{Eq. S1})$$

The activation energy of  $\alpha(T)$  of 21.3 ( $\pm 15\%$ ) kJ/mol and the constant contribution  $\alpha_0$  of  $8 (\pm 0.5) \cdot 10^{-5} \text{ s}^{-1} \text{ mW}^{-2}$  was determined from the fit (Figs. 5 and S5). Fig. S5 shows the Arrhenius plot for the  $\alpha(T)$  coefficient with the constant contribution subtracted.

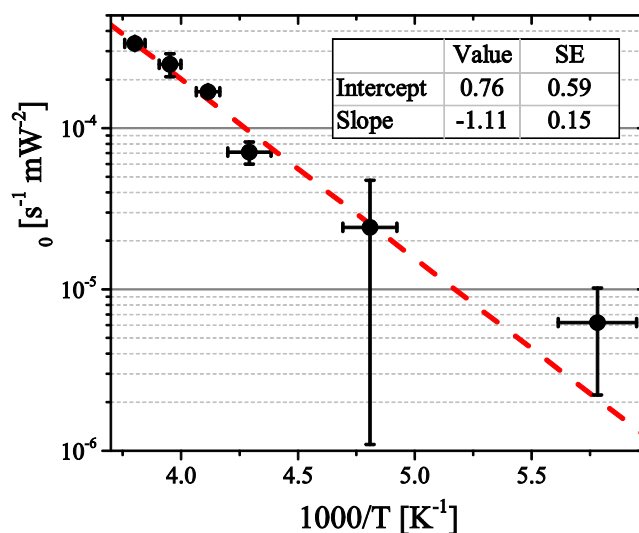


FIGURE S5. Arrhenius plot of the  $\alpha$  coefficient with the constant contribution ( $\alpha_0$ ) subtracted. The line is the fit by the thermal activation law ( $R^2 = 0.98$ ). Error bars denote standard error.

## SUPPORTING REFERENCES

1. Kakita, M., V. Kaliaperumal, and H. Hamaguchi. 2012. Resonance Raman quantification of the redox state of cytochromes b and c in-vivo and in-vitro. *J. Biophotonics*. 5:20–24.
2. Hu, S., I. K. Morris, ..., T. G. Spiro. 1993. Complete assignment of cytochrome c resonance Raman spectra via enzymatic reconstruction with isotopically labeled hemes. *J. Am. Chem. Soc.* 115:12446–12458.
3. De Gelder, J., K. De Gussem, ..., L. Moens. 2007. Reference database of Raman spectra of biological molecules. *J. Raman Spectrosc.* 38:1133–1147.
4. Mayo, D. W., F. A. Miller, and R. W. Hannah. 2004. Course Notes on the Interpretation of Infrared and Raman Spectra. John Wiley & Sons, Hoboken, NJ.
5. Prescott, B., W. Steinmetz, and G. J. Thomas, Jr. 1984. Characterization of DNA structures by laser Raman spectroscopy. *Biopolymers*. 23:235–256.
6. Pliss, A., A. N. Kuzmin, ..., P. N. Prasad. 2010. Nonlinear optical imaging and Raman microspectrometry of the cell nucleus throughout the cell cycle. *Biophys. J.* 99:3483–3491.
7. Uzunbajakava, N., A. Lenferink, ..., C. Otto. 2003. Nonresonant Raman imaging of protein distribution in single human cells. *Biopolymers*. 72:1–9.